Int. J. Environ. Sci. Technol. (2016) 13:1573–1580
DOI 10.1007/s13762-016-0973-8

ORIGINAL PAPER

# Heterogeneous $C_{16}Zn_8O_8$ nanocluster as a selective CO/NO nanosensor: computational investigation

**Saeed Soleimani Gorgani[1] · M. Nouraliei[1] · Sara Soleimani Gorgani[1]**

Received: 25 June 2015 / Revised: 30 November 2015 / Accepted: 23 February 2016 / Published online: 7 April 2016


**Abstract** Density functional theory (DFT) calculations were employed to investigate the effects of adsorption of toxic carbon monoxide (CO) and nitrogen monoxide (NO) molecules on heterogeneous $C_{16}Zn_8O_8$ nanocage. A detailed analysis of the energetic, geometry, and electronic structure of various CO and NO adsorptions on the cluster surface was performed. It has been shown that CO molecule was adsorbed on the surface of the cluster resulting in more stable complex system, while NO molecule adsorption led to less stable system. These processes also changed the electronic properties of the cluster by reducing the HOMO/LUMO energy gap after adsorption process. Since this phenomenon led to an increment in the electrical conductivity of the cluster at a definite temperature, the $C_{16}Zn_8O_8$ was transformed to a stronger semiconductor substance upon the CO and NO adsorption. We believe that this research may be helpful in the several fields study such as sensor and catalyst investigation.

**Keywords** Adsorption · Carbon monoxide · Nitrogen monoxide · Nanocage · Electrical conductivity

## Introduction

Air pollution is one of the most significant problems for countries across the globe (Zhuiykov et al. 2001; Chang et al. 2001). A wide range of industries release toxic materials and gases into the environment in amounts that can pose risk to human health (Gupta and Nayak 2012; Mittal et al. 2009). Since the air pollution is a mixture of solid particles and gases in the air comprised of hazardous and harmful vapors, the environmental gas monitoring and controlling is now recognized as an important area for clean atmosphere and human body (Lu et al. 2005).

Carbon monoxide (CO) and nitrogen oxide (NO) are of the extremely toxic molecules among the air pollutants and in human daily life. Therefore, effective methods to detect and decrease the CO and NO content in the atmosphere have been highly requested for environmental measurements and controls (Santucci et al. 2003; Lee et al. 1999). Among different methods, adsorbents such as various naturally available adsorbents like wool, olive cake, sawdust, pine needles, almond shells, cactus leaves, charcoal used tyres, soot, hazelnut shell, coconut shell charcoal, banana peel, seaweed, dead fungal biomass, cyanobacterium, and green alga have been used for the removal of some pollutants from the environment (Gupta et al. 1999, 2001, 2009; Gupta and Ali 2004; Ali and Gupta 2007; Gupta and Rastogi 2008, 2009; Singh et al. 2007).

However, many of these naturally available adsorbents have low gas adsorption capacity and slow process kinetics. Thus, there is a need to develop innovative gas adsorbents useful both for industry and for the environment.

Due to unique properties including very large percentage of atoms at interfaces, quantum confinement effects, and very sensitive electronic properties (Beheshtian et al.

This work has been carried out at Islamic Republic of Iran in the summer of 2015.

**Electronic supplementary material** The online version of this article (doi:10.1007/s13762-016-0973-8) contains supplementary material, which is available to authorized users.

✉ Sara Soleimani Gorgani
sarasoleimani240@yahoo.com

[1] Young Researchers and Elite Club, Central Tehran Branch, Islamic Azad University, Tehran, Iran

2011a), nanostructures have already been investigated as promising adsorbents for various organic pollutants and metal ions and can be easily modified by chemical treatment to increase their adsorption capacity (Chen et al. 2009).

Nanostructured materials are a new class of materials which provide one of the greatest potentials for improving performance and extended capabilities of new devices in a number of biological and non-biological sectors. Designing and preparing of new nanostructured materials specially, fullerene-related materials have attracted considerable attention due to their novel physical and chemical properties (Hirsch 1994; Fang et al. 2008; Trani et al. 2009). A fullerene is a molecule of carbon which can be in the form of a hollow sphere, ellipsoid, tube, and many other shapes. The first fullerene molecule ($C_{60}$) was discovered in 1985 by Richard Smalley, Robert Curl, James Heath, Sean O' Brien, and Harold Kroto at Rice University. The discovery of fullerenes greatly expanded the number of carbon allotropes, which were limited to graphite, diamond, and amorphous carbon such as soot and charcoal. Fullerenes have been extensively used in the form of nanocage structures, nanotubes, nanocapsules, and nanopolyhedral in electronics and nanotechnology and for several biomedical applications including the design of high-performance MRI contrast agents, X-ray imaging contrast agents, photodynamic therapy and drug and gene delivery.

Recently, many researches have been dedicated in order to identify, simulate, and fabricate $(XY)_n$ nanostructures in which the X and Y are atoms except carbon such as $(BN)_n$, $(MgO)_n$, $(AlN)_n$, and $(ZnO)_n$. $(XY)_n$ nanostructured metal oxides such as zinc oxide $(ZnO)_n$ are currently of great interest due to their significance in industrial catalysis, nanoball bearings, nano-optical magnetic devices, gas sensors, and biotechnology (Ghenaatian et al. 2013; Gao et al. 2004). $(ZnO)_n$ nanostructures are so effective for a wide range of reactions that are important in both pollution control and chemical synthesis (Barsan et al. 2007). ZnO is known as metal oxide semiconductor with high sensitivity toward several toxic and combustible gases (Bae and Choi 1999).

During the last decade, much research interest has been focused on the synthesis of fullerene-related materials due to their novel properties (Saleh 2011; Gupta et al. 2012). Also, much of the recent published research has been directed at ZnO nanocluster structures both theoretically and experimentally (Al-Sunaidi and Goumri-Said 2011; Joicy et al. 2014; Saravanan et al. 2015a, b), but very little effort has thus far been put toward heterogeneous $C_nZn_nO_n$ nanoclusters. ZnO nanostructures are exploited as gas sensor due to their dramatic changes in the conductivity of nanoclusters after gas adsorption. However, carbon fullerene materials demonstrate greater conductivity than ZnO nanoclusters after adsorption process. For this reason, the creation of heterogeneous fullerene-like nanoclusters includes of C, Zn, and O atoms and can have a greater impact on the amount of surface conductivity. Here, the first simulation of the interaction between CO and NO molecules on heterogeneous $C_{16}Zn_8O_8$ nanocage is reported based on theoretical investigation. The main issues to be clarified by the present study include: (1) the place of CO and NO upon the interaction and (2) the effects of CO and NO adsorption on the electronic properties of $C_{16}Zn_8O_8$. Our results can be helpful for direct experimental explorations of new heterogeneous nanostructured materials for catalysis or sensor applications.

## Computational methods

Geometry optimizations, molecular electrostatic potential (MEP), natural bonding orbital (NBO) analysis (Glendening et al. 2013) and density of states (DOS) analyses were performed on $C_{16}Zn_8O_8$ and different NO- or CO-$C_{16}Zn_8O_8$ configurations at the $O_3$LYP/6-31G* level of theory. $O_3$LYP is a hybrid generalized gradient approximation (GGA) functional, which includes a mixture of Hartree–Fock exchange with DFT exchange correlation. According to the previous studies in the area of nanostructured materials, it has been established that the $O_3$LYP is a very good method to determine the dispersion, van der Waals forces, and gap of neutral and charged molecules (León and Pacheco 2011; Xu and Goddard 2004), and therefore, it has been adopted to determine the gap parameter of the molecules studied in this investigation. As shown previously that 6-31G* is the most optimal basis set from the standpoints of calculation time and accuracy (Beheshtian et al. 2012b), we selected it as the confirmed basis set in this study. GaussSum program (O'Boyle et al. 2008) was used to obtain DOS results. In addition, the vibrational frequencies were calculated at the $O_3$LYP/6-31G* level to confirm that all the stationary points adapted true minima on the potential energy surface. All calculations reported here were carried out using a locally modified version of the GAMESS electronic structure program (Schmidt et al. 1993). A very important parameter to determine the amount of the adhesion of a chemical species onto the surface of particles in gas sensors is the correct description of adsorption in which an adsorbate is adhered to the surface of the adsorbent by means of physical, chemical, or electrostatic forces (Saleh and Gupta 2014). Exploiting nanostructured materials as adsorbent in the adsorption process in gas sensors demonstrates a serious challenge for theoretical and experimental studies in the case of bonding of simple molecules to the nanostructure surfaces (Eid and Ammr 2011; Beheshtian et al. 2012d; Erdogan et al. 2010). We have defined the adsorption energy ($E_{ads}$) of CO and NO as follows:

$$E_{ads} = E_{adsorbate/cluster} - E_{adsorbate} - E_{cluster} \quad (1)$$

where $E_{adsorbate/cluster}$ is the total energy of CO and NO molecules adsorbed on the surface of nanocage and $E_{cluster}$ and $E_{adsorbate}$ are the total energies of the pristine cluster and CO and NO molecules, respectively. By the definition, negative value of $E_{ads}$ corresponds to exothermic adsorption processes (Beheshtian et al. 2012a).

## Results and discussion

At first, structure of pure heterogeneous $C_{16}Zn_8O_8$ consisted of six squares, six hexagons, and two octagons, which was optimized as a basis model. DOS plot of the pristine $C_{16}Zn_8O_8$ in Fig. 1 indicated that it was a semiconductive substance due to the difference in energy between the highest occupied molecular orbital (HOMO) and the lowest unoccupied molecular orbital (LUMO). The $E_g$ (HOMO–LUMO gap) of the $C_{16}Zn_8O_8$ nanocluster was calculated to be about 1.22 eV (Fig. 1).

### Adsorption energy determination

In order to obtain the most stable configuration for CO and NO adsorption, we considered all the possible adsorption sites: on top of the surface Zn, O, and C atoms in all sides of the cluster surface. However, upon optimization only two local minima were obtained for CO and NO adsorbed on the cluster. In Fig. 2, we reported the optimized structures for both adsorbed systems including the carbon head of CO and oxygen head of NO on top of a Zn atom of the cluster with distance of 2.04 and 2.01 Å. Our calculations showed that the configurations for both CO and NO adsorption were exothermic processes with negative $E_{ads}$ −0.74 and −2.1 eV, respectively. As shown in Table 1, the charge transfer from CO and NO toward the nanocluster was about −0.053 and −0.637 |e|, respectively. Detailed information including values of $E_{ads}$, NBO charge transfer, and the $\Delta E_g$ (change of $E_g$ of cluster upon the adsorption process) is listed in Table 1.

### Molecular electrostatic potential analysis

In the next step, we decided to explore the adsorption interaction between CO and NO molecules with heterogeneous $C_{16}Zn_8O_8$ nanocluster. So we performed the MEP calculations which can explain the charge distribution. CO and NO cases were selected for the MEP computations on the $C_{16}Zn_8O_8$ surface. MEP is the molecular electronic potential surface generated by the charge distribution of the molecule, which at an atomic site is defined as follows:

$$V(r) = \sum_A \frac{Z_A}{|R_A - r|} - \int \frac{\rho(r')dr'}{|r' - r|} \quad (2)$$

$Z_A$ is the charge on nucleus $A$, located at $R_A$. The sign of $V(r)$ depends on whether the effects of the nuclei or the electrons are dominant at any point (Beheshtian et al. 2011b). So far, the MEP has frequently been used for the interpretation of the electrical properties of various materials (Peralta-Inga et al. 2003; Ahmadi et al. 2011; Politzer et al. 2005, 2001). MEP plots in Fig. 3 showed that the Zn atoms were positively charged, (blue colors), while the O and C atoms of the cluster were negatively charged (red colors). It evidences a charge transferring from the Zn atoms to the O and C ones resulting in ionic bonds in nanocluster surface. On the other hand, as shown in Fig. 3 a, the C atom of the CO was more negative than its O atom; therefore, it was predicted that the electron-rich C atom of CO should attack the electron-poor Zn atom of the cluster. Figure 3d shows that after adsorption process, the CO fragment was more positive supporting a charge transferring from CO to the cluster due to a strong

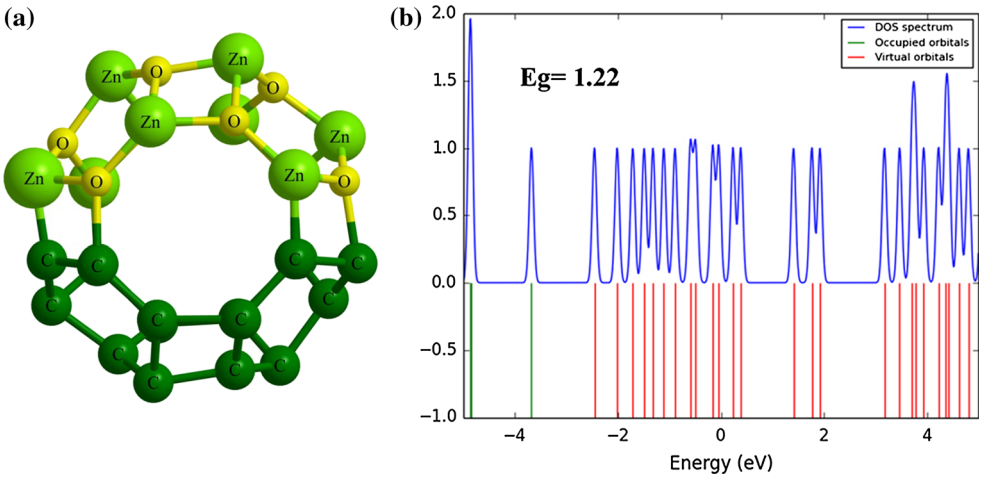


**Fig. 1** **a** Optimized structure of $C_{16}Zn_8O_8$ nanocluster, and **b** its DOS plot

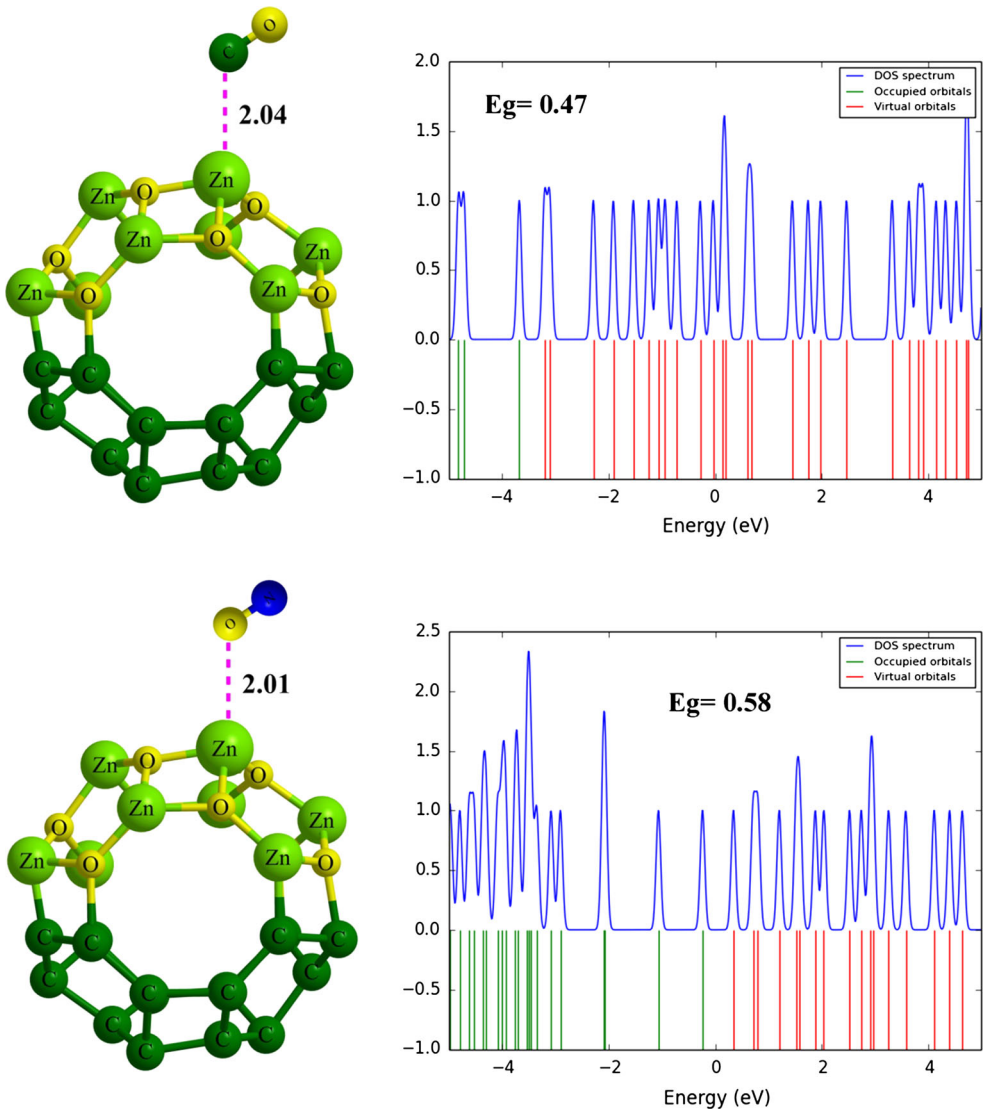


**Fig. 2** Model for adsorption of CO and NO on $C_{16}Zn_8O_8$ and their DOSs. Distances are in Å

**Table 1** Adsorption energy ($E_{ads}$) of CO and NO molecules on the $C_{16}Zn_8O_8$ nanocluster, the charge on the molecule after its adsorption ($Q_T$) on the cluster, the HOMO–LUMO energies, the HOMO–LUMO energy gaps ($E_g$), and the change of nanocluster HOMO–LUMO gap ($\Delta E_g$) upon the adsorption processes

| Configuration | $E_{ads}$ | $Q_T$ (e)[a] | HOMO | LUMO | $E_g$ | $\Delta E_g$ |
|---|---|---|---|---|---|---|
| $C_{16}Zn_8O_8$ | – | – | −0.13518 | −0.09022 | 1.22 | – |
| $C_{16}Zn_8O_8$-CO | −0.74 | −0.053 | −0.13520 | −0.11776 | 0.47 | 0.75 |
| $C_{16}Zn_8O_8$-NO | −2.1 | −0.637 | −0.00864 | 0.01269 | 0.58 | 0.64 |

[a] Q is defined as the total NBO charge transferring between adsorbed molecules and cluster

interaction. In this case, the total charge of complex was zero value. In contrast, in the interaction between NO and the cluster, the O head of NO molecule interacted with Zn atom of the cluster, creating a chemical bond between the O atom of NO and Zn atom of the heterogeneous $C_{16}Zn_8O_8$ nanocluster due to high $E_{ads}$ (Table 1). After adsorption process between NO and the $C_{16}Zn_8O_8$, the total charge of complex showed −1 value which can be seen in Fig. 3 e by more red color.

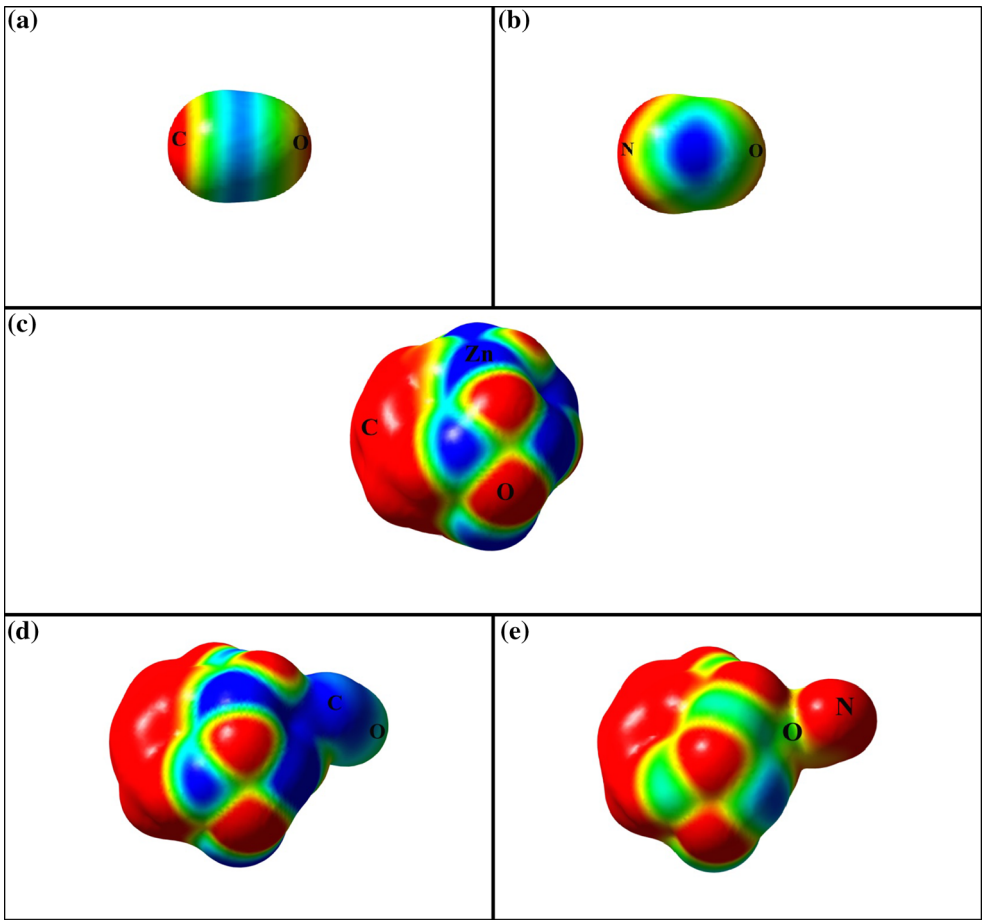


**Fig. 3** Calculated molecular electrostatic potential surfaces for **a** CO (carbon monoxide), **b** NO (nitrogen monoxide), **c** clean heterogeneous $C_{16}Zn_8O_8$, **d** CO adsorbed on the cluster, **e** NO adsorbed on the cluster. The surfaces are defined by the 0.0004 electrons/b3 contour of the electronic density. Color ranges, in a.u.: *blue*, more positive than 0.050; *red*, more negative than –0.050

## HOMO–LUMO gap analysis

Additionally to explore the CO and NO interaction with the Zn atom of cluster, we offered suite plots of the HOMO (highest occupied molecular orbital) and LUMO (lowest unoccupied molecular orbital) for the present $C_{16}Zn_8O_8$ nanocluster with and without the CO and NO molecules. HOMO–LUMO profiles in Fig. 4 revealed that in CO adsorption process the LUMO was more localized on the Zn atoms of the cluster in energy level of −0.09022 eV. On the other hand, it has previously been shown that the HOMO of CO molecule was located on the C atom (Beheshtian et al. 2012c), so it approached the Zn atom of cluster from C head. After CO adsorption process, the LUMO was more localized on Zn atom of the cluster and adsorbed CO molecule. Energy level of LUMO in this case was about −0.1177 eV, indicating that it has became more stable upon the CO adsorption. On the other hand, as shown in Fig. 4, the HOMO of pure and CO-adsorbed cluster was more localized on the C atoms of the cluster in energy levels of −0.13518 and −0.13520 eV, respectively. It can be seen that the HOMO was not efficiently changed upon the adsorption process, indicating that the HOMO was not participated to the CO adsorption process. In NO adsorption interaction, the LUMO and HOMO changed from −0.1177 to 0.01269 eV and −0.13518 to −0.00864 eV, respectively, indicating that both HOMO and LUMO have became less stable upon the NO adsorption.

## Density of state analysis

The total electronic density of states (DOS) of the molecules/nanocluster complex was calculated to verify the effects of the adsorption of molecules on the nanocluster electronic properties (Fig. 2). As a result, the system became more semiconductor-like ($E_g$ nanocluster = 1.22 eV → $E_g$ CO/nanocluster and NO/nanocluster = 0.47 and 0.58 eV, respectively) for the most stable configuration. This occurrence was expected to bring

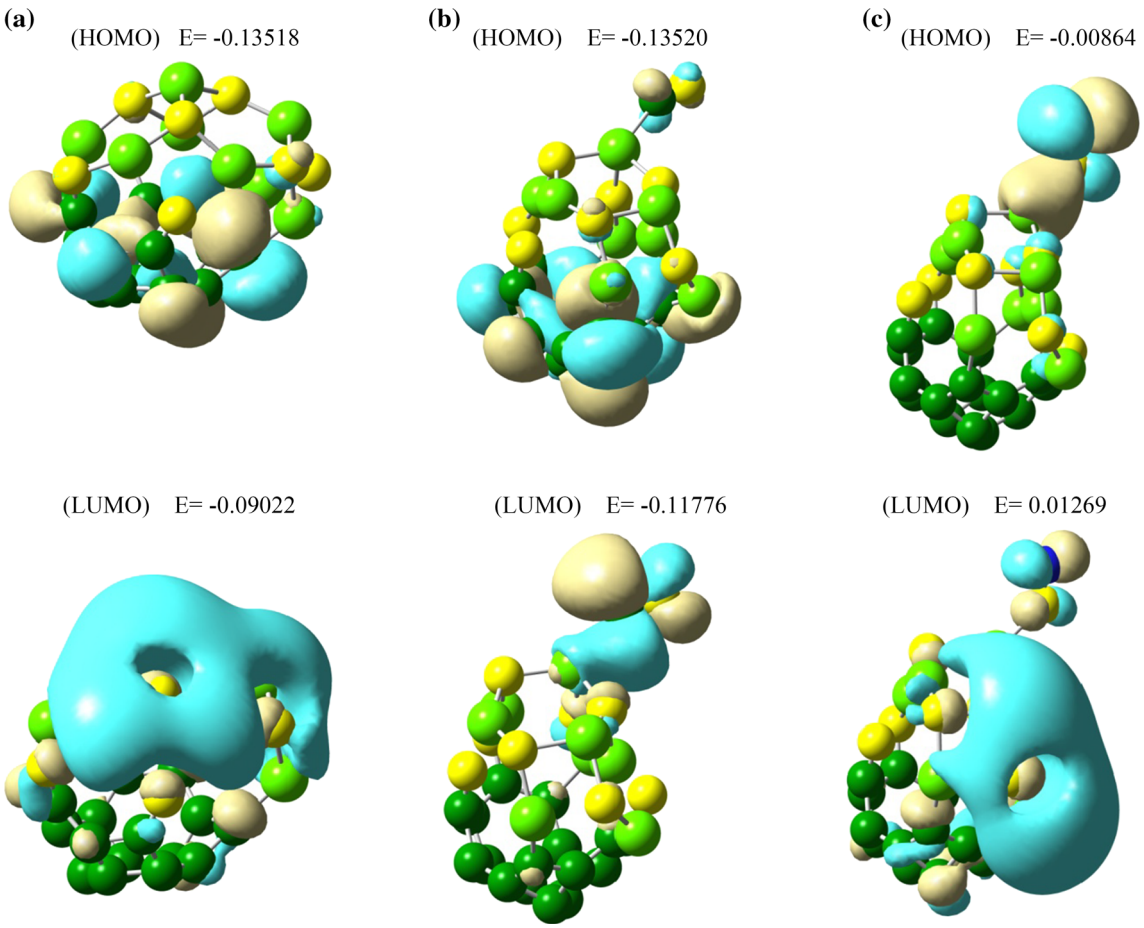


**Fig. 4** HOMO and LUMO profiles of the clean **a,** CO-adsorbed $C_{16}Zn_8O_8$ **b** and CO-adsorbed $C_{16}Zn_8O_8$ **c**. Energies are in eV

about obvious change in the electrical conductivity of cluster according to the following equation (Li 2006):

$$\sigma \propto exp\left(\frac{-E_g}{2kT}\right) \quad (3)$$

where $\sigma$ is the electrical conductivity and $k$ is the Boltzmann′s constant. According to Eq. 3, the smaller $E_g$ at a room temperature leads to the higher electrical conductivity. However, the $E_g$ of the both CO/$C_{16}Zn_8O_8$ and NO/$C_{16}Zn_8O_8$ complexes was reduced, compared to that of the clean cluster (Table 1). As the conductivity was exponentially correlated with negative value of $E_g$, it was expected that it became larger as the $E_g$ was reduced. It demonstrated the high sensitivity of the electronic properties of $C_{16}Zn_8O_8$ toward the adsorption of CO molecule. We thought that $C_{16}Zn_8O_8$ could transform the presence of the CO molecule directly into an electrical signal and, therefore, could be potentially used in CO sensor devices. In contrast, despite the high $E_{ads}$ of $C_{16}Zn_8O_8$ for NO molecule, because of chemical binding that occurred through the adsorption process which reduced the stability of the complex after adsorption, the $C_{16}Zn_8O_8$ could not be used as a good NO gas sensor. Hence, it could be deduced that $C_{16}Zn_8O_8$ nanocage selectively functions as a gas sensor device between CO and NO gases. Figure 5 is a schematic diagram which shows the process and the mechanism of the main goal of the study. The light of the lamp is relative to conductivity of the cluster which is affected by CO/NO adsorption. As shown in Fig. 5, after CO adsorption, the lamp shows more light which proves more conductivity of cluster under CO adsorption.

## Conclusion

We have investigated carbon monoxide (CO) and nitrogen monoxide (NO) adsorption on heterogeneous $C_{16}Zn_8O_8$ using computational method. It was found that the CO could be adsorbed on $C_{16}Zn_8O_8$ via chemisorptions mechanism with $E_{ads}$ of −0.74 eV, resulting in more stability of the complex system. Indeed, the CO adsorption reduced the $E_g$ of the cluster which made it a sensitive sensor. Despite the high NO $E_{ads}$, the $E_g$ changed slightly and the system became less stable after adsorption process.

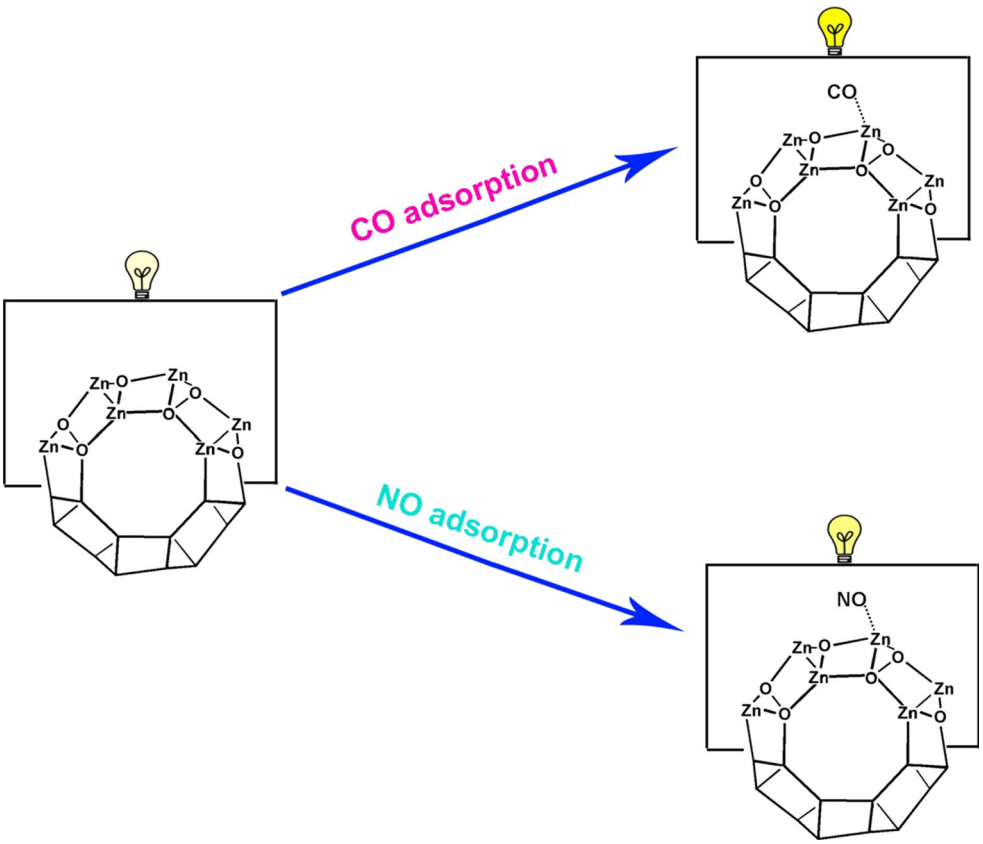


**Fig. 5** Schematic diagram to show the CO/NO adsorption mechanisms and their effects on nanocluster conductivity which can be used as electrical sensor

Totally, it must be concluded that $C_{16}Zn_8O_8$ acts selectively against the CO and NO gaseous molecules. We hope that our results be helpful for sensor and adsorption fields.

## References


Ahmadi A, Kamfiroozi M, Beheshtian J, Hadipour N (2011) The effect of surface curvature of aluminum nitride nanotubes on the adsorption of $NH_3$. Struct Chem 22:1261–1265

Ali I, Gupta VK (2007) Advances in water treatment by adsorption technology. Nat Protoc 1:2661–2667

Al-Sunaidi A, Goumri-Said S (2011) Investigating the adsorption of $H_2O$ on ZnO nanoclusters by first principle calculations. Chem Phys Lett 507:111–116

Bae HY, Choi GM (1999) Electrical and reducing gas sensing properties of ZnO and ZnO–CuO thin films fabricated by spin coating method. Sens Actuators B Chem 55:47–54

Barsan N, Koziej D, Weimar U (2007) Metal oxide-based gas sensor research: How to? Sens Actuators B Chem 121:18–35

Beheshtian J, Bagheri Z, Kamfiroozi M, Ahmadi A (2011a) Toxic CO detection by $B_{12}N_{12}$ nanocluster. Microelectron J 42:1400–1403

Beheshtian J, Kamifiroozi M, Bagheri Z, Ahmadi A (2011b) Computational study of CO and NO adsorption on magnesium oxide nanotubes. Phys E 44:546–549

Beheshtian J, Ahmadi Peyghan A, Bagheri Z (2012a) Adsorption and dissociation of $Cl_2$ molecule on ZnO nanocluster. Appl Surf Sci 258:8171–8176

Beheshtian J, Bagheri Z, Kamfiroozi M, Ahmadi A (2012b) A comparative study on the $B_{12}N_{12}$, $Al_{12}N_{12}$, $B_{12}P_{12}$ and $Al_{12}P_{12}$ fullerene-like cages. J Mol Model 18:2653–2658

Beheshtian J, Bagheri Z, Kamfiroozi M, Ahmadi A (2012c) A theoretical study of CO adsorption on aluminum nitride nanotubes. Struct Chem 23:653–657

Beheshtian J, Soleymanabadi H, Kamfiroozi M, Ahmadi A (2012d) The $H_2$ dissociation on the BN, AlN, BP and AlP nanotubes:a comparative study. J Mol Model 18:2343–2348

Chang H, Lee JD, Lee SM, Lee YH (2001) Adsorption of $NH_3$ and $NO_2$ molecules on carbon nanotubes. Appl Phys Lett 79:3863–3865

Chen L, Xu C, Zhang X-F, Zhou T (2009) Raman and infrared-active modes in MgO nanotubes. Physica E 41:852

Eid KM, Ammr HY (2011) Adsorption of $SO_2$ on Li atoms deposited on MgO (1 0 0) surface: DFT calculations. Appl Surf Sci 257:6049–6058

Erdogan R, Ozbek O, Onal I (2010) A periodic DFT study of water and ammonia adsorption on anatase $TiO_2$ (0 0 1) slab. Surf Sci 11–12:1029–1033

Fang T-H, Wang TH, Lu D-M, Lien W-C (2008) Structural characteristics of carbon nanostructures synthesized by ECR-CVD. Microelectron J 39:1600–1604

Gao XD, Li XM, Yu WD (2004) Synthesis and optical properties of ZnO nanocluster porous films deposited by modified SILAR method. Appl Surf Sci 229:275–281

Ghenaatian HR, Baei MT, Hashemian S (2013) $Zn_{12}O_{12}$ nano-cage as a promising adsorbent for $CS_2$ capture. Superlattice Microst 58:198–204

Glendening ED, Landis CR, Weinhold F (2013) NBO 6.0: natural bond orbital analysis program. J Comput Chem 34:1429–1437

Gupta VK, Ali I (2004) Removal of lead and chromium from wastewater using bagasse fly ash—sugar industry waste. J Colloid Interface Sci 271:321–328

Gupta VK, Nayak A (2012) Cadmium removal and recovery from aqueous solutions by novel adsorbents prepared from orange peel and $Fe_2O_3$ nanoparticles. Chem Eng J 180:81–90

Gupta VK, Rastogi A (2008) Sorption and desorption studies of chromium(VI) from nonviable cyanobacterium nostoc muscorum biomass. J Hazard Mater 154:347–354

Gupta VK, Rastogi A (2009) Biosorption of hexavalent chromium by raw and acid treated green alga Oedogonium hatei from aqueous solutions. J Hazard Mater 163:396–402

Gupta VK, Mohan D, Sharma S, Park KT (1999) Removal of chromium(VI) from electroplating industry wastewater using bagasse fly ash—a sugar industry waste material. Environmentalist 19:129–136

Gupta VK, Gupta M, Sharma S (2001) Process development for the removal of lead and chromium from aqueous solutions using red muddan aluminium industry waste. Water Res 35:1125–1134

Gupta VK, Carrott PJM, Ribeiro Carrott MML, Suhas (2009) Low cost adsorbents: growing approach to waste-water treatment—a review. Crit Rev Environ Sci Technol 39:783–842

Gupta VK, Imran A, Saleh TA, Nayak A, Agarwal Sh (2012) Chemical treatment technologies for waste–water recycling—an overview. RSC Adv 2:6380–6388

Hirsch A (1994) The chemistry of the fullerenes. Thieme, New York

Joicy S, Saravanan R, Prabhu D, Ponpandian N, Thangadurai P (2014) $Mn^{2+}$ ion influenced optical and photocatalytic behaviour of Mn-ZnS quantum dots prepared by a microwave assisted technique. RSC Adv 4:44592

Lee D-S, Han S-D, Huh J-S, Lee D-D (1999) Nitrogen oxides-sensing characteristics of $WO_3$-based nanocrystalline thick film gas sensor. Sens Actuators B Chem 60(1):57–63

León A, Pacheco M (2011) Electronic and dynamics properties of a molecular wire of graphane nanoclusters. Phys Lett A 375(2011):4190–4197

Li S (2006) Semiconductor physical electronics, 2nd edn. Springer, Berlin

Lu J, Nagase S, Maeda Y, Wakahara T, Nakahodo T, Akasaka T, Yu D, Gao Z, Han R, Ye H (2005) Adsorption configuration of $NH_3$ on single–wall carbon nanotubes. Chem Phys Lett 405:90–92

Mittal A, Kaur D, Malviya A, Mittal J, Gupta VK (2009) Adsorption studies on the removal of coloring agent phenol red from wastewater using waste materials as adsorbents. J Colloid Interface Sci 337:345–354

O'Boyle NM, Tenderholt AL, Langner KM (2008) cclib: a library for package independent computational chemistry algorithms. J Comput Chem 29:839–845

Peralta-Inga Z, Lane P, Murray JS, Boyd S, Grice ME, Connor CJO, Politzer P (2003) Characterization of surface electrostatic potentials of some (5,5) and (n,1) carbon and boron/nitrogen model nanotubes. NanoLetters 3:21

Politzer P, Grice ME, Murray JS (2001) Electronegativities, electrostatic potentials and covalent radii. J Mol Struct (Theochem) 69:549

Politzer P, Lane P, Murray JS, Concha MC (2005) Comparative analysis of surface electronic potentials of carbon, boron/nitrogen and carbon/boron/nitrogen model nanotubes. J Mol Model 1:11

Saleh TA (2011) The influence of treatment temperature on the acidity of MWCNT oxidized by $HNO_3$ or a mixture of $HNO_3$/$H_2SO_4$. Appl Surf Sci 257:7746–7751

Saleh TA, Gupta VK (2014) Processing methods, characteristics and adsorption behavior of tire derived carbons: a review. Adv Colloid Interface Sci 211:93–101

Santucci S, Picozzi S, Di Gregorio F, Lozzi L, Cantalini C, Valentini L, Kenny JM, Delley B (2003) $NO_2$ and CO gas adsorption on carbon nanotubes: experiment and theory. J Chem Phys 119(20):10904

Saravanan R, Mansoob Khan M, Gupta VK, Mosquera E, Gracia F, Narayanan V (2015a) ZnO/Ag/CdO nanocomposite for visible light-induced photocatalytic degradation of industrial textile effluents. J Colloid Interface Sci 452:126–133

Saravanan R, Mansoob Khan M, Gupta VK, Mosquera E, Gracia F, Narayanan V, Stephen A (2015b) ZnO/Ag/$Mn_2O_3$ nanocomposite for visible light-induced industrial textile effluent degradation, uric acid and ascorbic acid sensing and antimicrobial activity. RSC Adv. 5:34645–34651

Schmidt MW, Baldridge KK, Boatz JA, Elbert ST, Gordon MS, Jensen JH, Koseki S, Matsunaga N, Nguyen KA, Su S, Windus TL, Dupuis M, Montgomery JA (1993) General atomic and molecular electronic structure system. J Comput Chem 14:1347–1363

Singh AK, Gupta VK, Gupta B (2007) Chromium(III) selective membrane sensors based on Schiff bases as chelating ionophores. Anal Chim Acta 585:171–178

Trani F, Caus-a M, Lettieri S, Setaro A, Ninno D, Barone V, Maddalena P (2009) Role of surface oxygen vacancies in photoluminescence of tin dioxide nanobelts. Microelectron J 40:236–238

Xu X, Goddard W (2004) The X3LYP extended density functional for accurate descriptions of nonbond interactions, spin states, and thermochemical properties. Proc Natl Acad Sci USA 101:2673–2677

Zhuiykov S, Wlodarski W, Li Y (2001) Nanocrystalline $V_2O_5$–$TiO_2$ thin-films for oxygen sensing prepared by sol-gel process. Sens Actuators B 77:484–490